A New 400-kD Protein from Isolated Adherens Junctions: Its Localization at the Undercoat of Adherens Junctions and at Microfilament Bundles such as Stress Fibers and Circumferential Bundles

Shoichiro Tsukita,* Masahiko Itoh,*‡ and Sachiko Tsukita*

*Department of Ultrastructural Research, The Tokyo Metropolitan Institute of Medical Science, Honkomagome 3-18-22, Bunkyo-ku, Tokyo 113, Japan; and ‡Department of Physics, School of Science and Engineering, Waseda University, Shinjuku-ku, Tokyo 169, Japan

Abstract. In the previous study, we succeeded in isolating the cell-to-cell adherens junctions from rat liver (Tsukita, S., and S. Tsukita. 1989. *J. Cell Biol.* 108:31–41.). In this study, we have obtained mAbs specific to the 400-kD protein, which was identified as one of the major constituents of the undercoat of isolated adherens junctions. Immune blot analyses showed that this protein occurs in various types of tissues. Immunofluorescence microscopy and immune electron microscopy have revealed that this protein is distributed not only at the undercoat of adherens junctions but also along actin bundles associated with the junction in nonmuscle cells: stress fibers in cultured fibroblasts and circumferential bundles in epithelial cells. The partially purified protein molecule looks like a slender rod ~400 nm in length. By virtue of its molecular shape, we have named this protein 'tenuin' (from Latin 'tenuis', thin or slender).

IN nonmuscle cells, motility and maintenance of cell shape are largely dependent on actin-based structures (14). These structures show a variety of morphologies: some are ordered arrays of actin filaments and others are random networks. Examples of the ordered arrays are stress fibers in cultured fibroblasts and circumferential bundles in epithelial cells (3, 25, 27, 36). These actin bundles can contract in combination with myosin molecules (13, 24). To understand the physiological roles of these bundles, it is prerequisite to know the molecular basis of the association between these bundles and plasma membranes. The attachment site is called adherens junction; it is subclassified into two types: cell-to-cell and cell-to-substrate (11). This junction is characterized by its well-developed undercoat, through which actin filaments are associated with plasma membranes (6, 8, 29). Because so far no biochemical enrichment procedure has been available for adherens junctions, the immunological approach was the only way to identify the components of the undercoat of adherens junctions. This type of approach revealed that some proteins such as vinculin (7, 10), talin (1, 2), α-actinin (18), filamin (9), and pp60^{src} (26, 28) were localized at the undercoat of the adherens junctions. Recently, we have succeeded in isolating the cell-to-cell adherens junction from rat liver and in identifying 10 major constituents of its undercoat, including vinculin, α-actinin, and actin (30). Among them, one of the major polypeptides, radixin (82 kD), has already been purified and characterized in vitro (31).

As a continuation of our recent work, we have attempted to analyze another major constituent of the undercoat of adherens junctions: the one with the highest molecular weight. In this study, we attempted to obtain mAbs specific to this high-molecular weight protein and analyzed in vivo localization of this protein. By virtue of its characteristic molecular shape (a slender rod-like structure), we refer to this protein as 'tenuin' (from Latin 'tenuis', thin or slender) in this paper.

Materials and Methods

mAb Production

The adherens junction was prepared from rat liver by the combination of homogenization, sucrose density gradient centrifugation, and NP-40 treatment, according to the method described previously (30). The low salt extract was obtained by dialysis of the adherens junction fraction against the extraction solution (1 mM EGTA, 0.5 mM PMSF, 1 μg/ml leupeptin, 2 mM Tris-HCl, pH 9.2), followed by centrifugation at 100,000 g for 60 min. The extract containing 250 μg of protein was lyophilized, and the powder obtained was solubilized in 200 μl of distilled water. This solution was used in immunogen at each injection.

mAbs were obtained essentially according to the procedure of Köhler et al. (15). BALB/c mice were immunized with the above immunogen as follows: day 1, intraperitoneally in CFA; day 14, intraperitoneally in CFA; day 28, intraperitoneally without adjuvant. 3 d after the final injection, the spleen was removed and the splenocytes were fused with mouse P3 myeloma cells. 50% polyethylene glycol (PEG 4000; E. Merck, Darmstadt, FRG) in RPMI-1640 was used as the fusogen. The initial fusion products were plated in four 24-well plates in hypoxanthine/aminopterin/thymidine

medium. 6 d after fusion, fusion plates were screened for antibody production on an ELISA assay. The low salt extract from adherens junction fraction was used for ELISA assay.

The wells that showed positive activity were immediately expanded and then plated out at clonal density (1.2 cell/well) in a 96-well dish together with feeder cells (thymus lymphocytes). 1 wk after cloning, wells with a single clone were tested for antibody with a double screening of the ELISA and the immune blotting analysis. The clones that produced antibodies specific to tenuin were expanded and cloned again.

The antibody-rich supernatant or ascites was used for immune blotting and immunohistochemistry. Selected clones were grown in mass culture and injected intraperitoneally into pristane-primed mice to produce ascites culture.

Gel Electrophoresis and Immune Blotting

SDS-PAGE was based on the discontinuous Tris-glycine system of Laemmli (16). The stain Coomassie brilliant blue R-250 or silver staining (silver staining kit; Wako, Tokyo, Japan) was used.

Immune blotting was performed by one-dimensional electrophoresis, followed by electrophoretic transfer to nitrocellulose sheets (33). Nitrocellulose sheets were treated with antibody followed by horseradish peroxidase-labeled goat anti-mouse IgG (Bio-Rad Laboratories, Richmond, CA), and the localization of peroxidase was detected by the reaction using diaminobenzidine in the presence of Ni and Co ions (5).

Immunohistochemistry

Light Microscopy. For indirect immunofluorescence microscopy of frozen sections, samples were frozen using liquid nitrogen, and the frozen sections (~10 μm thick) were cut in a cryostat, mounted on glass slides, air-dried, and fixed in 95% ethanol at 4°C for 30 min and in 100% acetone at room temperature for 1 min. After being rinsed in PBS (150 mM NaCl, 10 mM phosphate buffer, pH 7.5) containing 1% BSA for 15 min, the sections were incubated with the supernatant rich in anti-tenuin mAb or with the ascite diluted with PBS containing 1% BSA for 30 min. They were then washed three times with PBS containing 1% BSA and 0.1% Triton X-100, followed by incubation with the FITC-conjugated goat anti-mouse IgM for 30 min. After being washed in PBS again, they were examined with a fluorescence microscope (Vanox-S; Olympus Corp. of America, Kanda, Tokyo, Japan).

For indirect immunofluorescence microscopy of cultured cells, rat 3Y1 cells and Madin-Darby bovine kidney (MDBK)[1] cells were cultured on cover glasses and fixed with 1% formaldehyde in PBS for 15 min. The fixed cells were treated with 0.2% Triton X-100 in PBS for 15 min and washed three times with PBS. After being soaked in PBS containing 1% BSA for 10 min, the sample was treated with the first antibody (anti-tenuin mAb or the mixture of anti-tenuin mAb and rabbit anti-vinculin antibody) for 1 h in a moist chamber. It was then washed with PBS containing 1% BSA three times, followed by incubation with the second antibody (FITC-conjugated goat anti-mouse IgM or the mixture of FITC-conjugated goat anti-mouse IgM and rhodamine-conjugated goat anti-rabbit IgG) for 30 min. In some experiments, rhodamine phalloidin was mixed with the second antibody. After incubation, the sample was washed with PBS three times and examined with an Olympus Vanox-S microscope.

For indirect immunofluorescence microscopy of the isolated bile canaliculi, the fraction rich in bile canaliculi (see reference 30) was put on the cover glass, air-dried, and fixed with 1% formaldehyde in PBS for 15 min. The fixed sample was soaked in PBS containing 1% BSA for 10 min and then processed as described above.

In all localization works, instead of the first antibody, some samples were incubated with PBS containing 1% BSA as control experiments. Because in all control experiments no staining was detected, we omitted micrographs from all figures that were controls for the specificity for the second antibodies. Anti-rat vinculin antibody was obtained in our laboratory as described previously (30). Anti-bovine desmoplakin I/II polyclonal antibody raised in guinea pigs was a generous gift from Dr. A. Kusumi (Tokyo University). FITC-conjugated goat anti-mouse IgM and rhodamine-conjugated goat anti-rabbit IgG were purchased from Cappel Laboratories (West Chester, PA). Rhodamine phalloidin was purchased from Molecular Probes, Inc. (Eugene, OR).

---

1. *Abbreviation used in this paper*: MDBK, Madin-Darby bovine kidney cells.

Electron Microscopy. For immunoelectron microscopy of the bile canaliculi, the fraction rich in bile canaliculi was obtained according to the method reported in the previous paper (30), and processed as described previously (31), except that samples were fixed with 1% formaldehyde for 10 min. When samples were doubly stained with mouse anti-tenuin and rabbit anti-vinculin antibody, goat anti-mouse IgM coupled to 10 nm gold and goat anti-rabbit IgG coupled to 15 nm gold (GAMIgM G10 and GARIgG G15) (Janssen Life Sciences Products, Piscataway, NJ) were used as the second antibodies.

For immunoelectron microscopy of cultured 3Y1 cells and MDBK cells, the cells were treated mainly according to the method developed by Langanger et al. (17). The cells on cover glass were extracted with 0.1% Triton X-100 in Pipes buffer 1 for 20 s at room temperature. The Pipes buffer 1 was composed of 137 mM NaCl, 5 mM KCl, 1.1 mM Na₂HPO₄, 0.4 mM KH₂PO₄, 4 mM NaHCO₃, 5.5 mM glucose, 5 mM Pipes, and 2 mM MgCl₂ (pH 6.1). The samples were fixed with 1% formaldehyde in Pipes buffer 2 (Pipes buffer 1 plus 2 mM EGTA) for 30 min, washed three times in Pipes buffer 2, permeated again with 0.5% Triton X-100 in Pipes buffer 2 for 30 min, and washed three times in Pipes buffer 2. The cells were then treated with TBS (20 mM Tris-buffered saline) containing 0.1% BSA for 20 min. These fixed and permeated cells were washed three times with TBS containing 0.1% BSA and then incubated with ascites containing mAb diluted 1:5,000 in TBS containing 0.1% BSA for 2 h at room temperature. After being washed three times in TBS containing 0.1% BSA, the samples were incubated in the second antibody (goat anti-mouse IgM) coupled to 10 nm gold (GAMIgM G10) (Janssen Life Science Products) diluted 1:50 in TBS containing 0.1% BSA overnight. They were then washed three times with TBS and twice in PBS, and fixed with 1% glutaraldehyde, 0.5% tannic acid and 0.1 M cacodylate buffer (pH 7.4). Fixation was continued overnight at 4°C, and then the samples were washed with 0.1 M sodium cacodylate buffer and postfixed with 1% OsO₄ in 0.1 M cacodylate buffer for 1 h at 4°C. After being rinsed in distilled water, samples were dehydrated in graded concentrations of ethanol and embedded in Epon 812. Thin sections were cut with a diamond knife, stained doubly with uranyl acetate, and lead citrate, and examined in an electron microscope (1200 EX; JEOL Tokyo, Japan) at an accelerating voltage of 100 kV.

Partial Purification of Tenuin

All procedures were performed at 4°C. Tenuin was purified from the low-salt extract of the adherens junction fraction. The adherens junction was prepared from rat liver, according to the method developed in the previous paper (30). The first low-salt extract (40 ml of 0.2 mg/ml) was obtained by dialysis of the adherens junction fraction against the extraction solution (1 mM EGTA, 0.5 mM PMSF, 1 μg/ml of leupeptin, 2 mM Tris-HCl, pH 9.2), followed by centrifugation at 100,000 g for 60 min. The pellet was resuspended in 20 ml of the extraction solution and dialyzed again against the same solution. The second extract (0.1 mg/ml) was obtained by centrifugation at 100,000 g for 60 min.

Preswollen DEAE cellulose was packed into a column (1 × 5 cm) and equilibrated with A buffer containing 10 mM Hepes, 1 mM EGTA, 0.1 mM DTT, 1 μg/ml of leupeptin, 1 mM PMSF (pH 7.5). The first and second low salt extracts were sequentially applied onto the DEAE cellulose column. The column was washed with 100 ml of A buffer followed by elution with 130 mM KCl/A buffer (pH 7.5) and 200 mM KCl/A buffer (pH 7.5). When fractions were assayed for tenuin by SDS-PAGE, tenuin was enriched in the 200 mM KCl/A buffer elute. This fraction was saved and further fractionated by gel filtration through Sepharose CL-4B (Pharmacia Fine Chemicals, Uppsala, Sweden) (2 × 45 cm) equilibrated with 100 mM KCl/A buffer (pH 7.5). Fractions enriched in tenuin were pooled by the assay with SDS-PAGE.

Low-angle Rotary-shadowing EM

The molecular shape of tenuin was analyzed by low-angle rotary-shadowing EM, mainly according to the method developed by Tyler and Branton (32). The solution containing partially purified tenuin was sprayed onto freshly cleaved mica. The droplets on the mica were dried at room temperature in a vacuum (1 × 10⁻⁶ Torr) in freeze-etch equipment (JFD 7000; JEOL) for 10 min. Platinum was then rotary-shadowed at an angle of 5°, followed by a coating from above with carbon. The replica was floated off on distilled water and picked up on formvar-filmed grids. The samples were examined in a JEOL 1200 EX electron microscope.
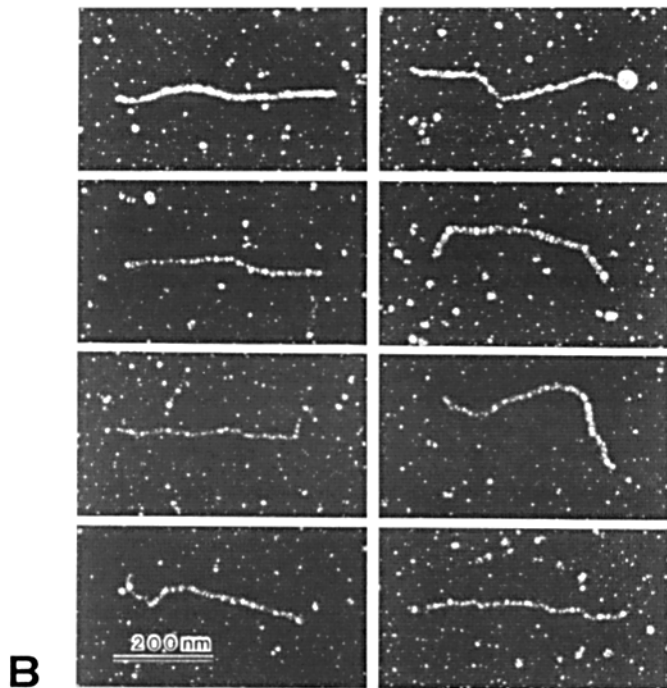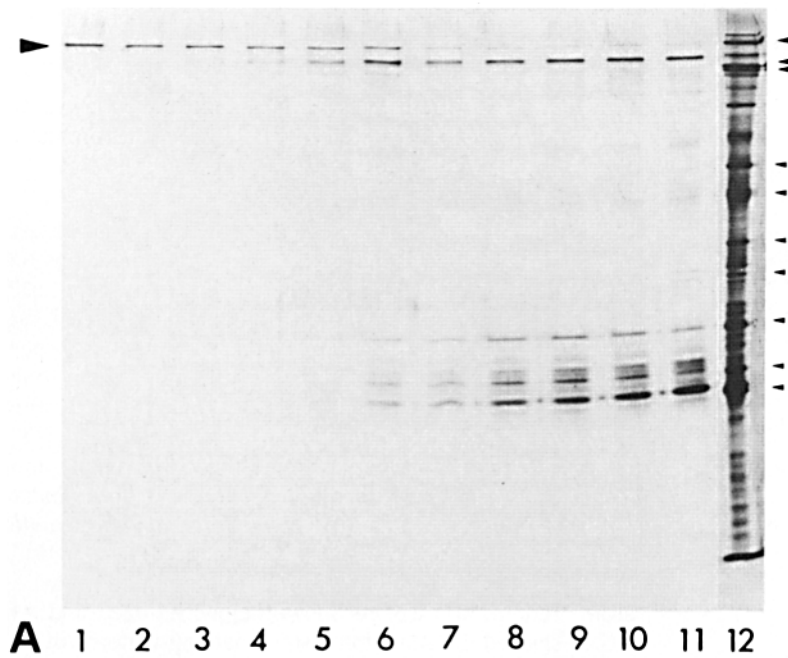
Figure 1. Partial purification of tenuin (*A*) and its molecular shape (*B*). (*A*) A 7.5% SDS-polyacrylamide gel of the fractions from Sepharose CL-4B column. In fractions *1–4*, tenuin (*large arrowhead*) is enriched. *Small arrowheads*, major constituents of the undercoat of adherens junctions (400, 240, 235, 130, 100, 82, 70, 55, 50, and 43 kD from the top). (*B*) Morphology of tenuin molecules in rotary-shadowed preparations. The tenuin molecule looks like a slender rod ∼400 nm long. Bar, 200 nm. ×70,000.

Results

Partial Purification of Tenuin and its Molecular Shape

As shown in our previous paper, 10 major polypeptides are identified in the low-salt extract of adherens junctions (30). In this study, we have attempted to obtain mAbs specific to one of these polypeptides with the highest molecular weight. Before mAb production, to study the molecular shape of this high-molecular weight protein, it was partially purified from the low-salt extract by the use of DEAE ion-exchange column chromatography and Sepharose CL-4B gel filtration column chromatography. It was enriched in the 200-mM KCl elute from a DEAE ion-exchange column, and the peak fractions
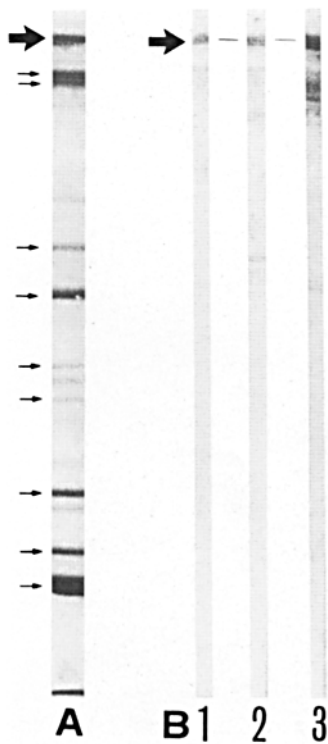
Figure 2. mAbs specific to tenuin. (*A*) Coomassie blue–stained gel (7.5%) of the low-salt extract of isolated adherens junctions. Tenuin (*large arrow*); the other major constituents (*small arrows*). Their molecular weights are (from the top) 400, 240, 235, 130 (vinculin), 100 (α-actinin), 82 (radixin), 70, 55, 50, and 43 kD (actin). (*B*) Immunoblot profiles with monoclonal antibodies; AJ-0222 (*1*), AJ-12249 (*2*), and AJ-43121 (*3*). All of these antibodies strongly blotted the band of tenuin (*large arrow*) and weakly blotted several lower molecular weight bands. The increase of these weakly blotted bands with time suggests that they are probably proteolytic degradation products.

like a slender rod ∼400 nm long (Fig. 1 *B*). Although some granular structures were seen to be associated, their positions were not constant, suggesting that these granular structures may be attributed to some contaminated proteins. By virtue of this characteristic molecular shape, this protein is called tenuin in this paper.

mAb Production

The spleen cells from four BALB/c mice immunized with a low-salt extract from isolated adherens junctions were fused with P3 myeloma cells. After the first cloning, in the ELISA assay using the low salt extract of adherens junctions, supernatants from 215 clones were positive. Among them, only three supernatants, AJ-0222, AJ-12249, and AJ-43121, were shown to be specific to tenuin in the immune blot assay (Fig. 2 *B*). Upon storage of samples, some bands with smaller molecular masses were stained. The increase of these bands with time suggested that they were probably proteolytic degradation products (see Fig. 2 *B*, lane *3*). These hybridomas were cloned twice by limiting dilution and grown as ascitic tumors in mice. As shown below, AJ-0222 and AJ-12249 showed the same interesting staining patterns in immunofluorescence microscopy, whereas no specific staining was detected by the use of AJ-43121. Results with AJ-0222 and AJ-12249 will be described in detail below.

Immune Blot Analysis of Tenuin in Various Types of Cells

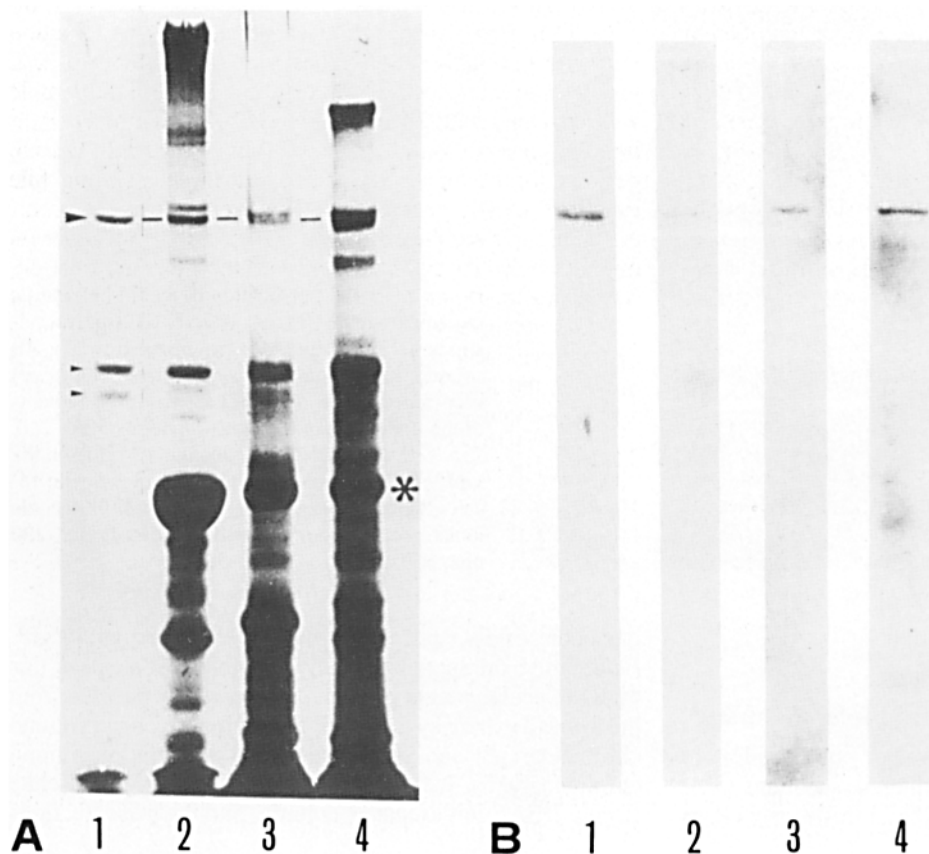The potential presence of tenuin in rat tissues was assessed by immune blot analysis. When the polypeptide composition

containing the high-molecular weight protein were pooled after gel filtration (Fig. 1 *A*). Using this partially purified protein, its molecular shape was analyzed by low-angle rotary-shadowing electron microscopy. The molecule looked

Figure 3. Immune blot analyses of the occurrence of tenuin in rat tissues. Lane *1*, low salt extract of adherens junctions (see reference 30); lane *2*, total cell homogenates of cardiac muscle; lane *3*, total cell homogenates of liver; lane *4*, total cell homogenates of 3Y1 (fibroblastic) cells. (*A*) Coomassie blue–stained gel (4%). In each tissue a band with the same molecular weight as tenuin is clearly identified (*large arrowhead*). Small arrowheads, 240- and 235 kD-protein; (∗) myosin heavy chain. (*B*) Accompanying immunoblots by the use of AJ-0222. Note the clear staining of a band of ∼400 kD (*arrow*) in all tissues examined.
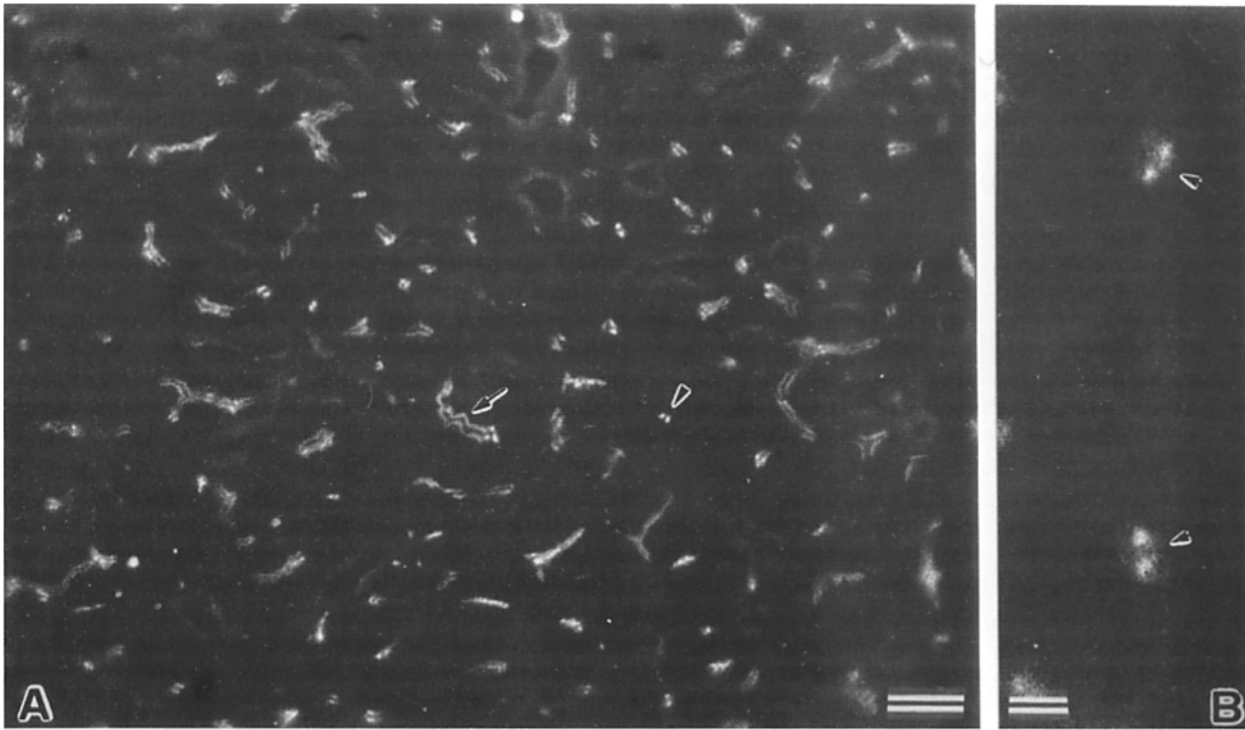
Figure 4. Indirect immunofluorescence images with AJ-0222 of the frozen section of rat liver. Intensive staining at the junctional complex along bile canaliculi can be detected. (*Arrow*) Longitudinal-section view of bile canaliculus; (*arrowhead*) cross-sectional view of bile canaliculus. At high magnification (*B*), in addition to a pair of intensively stained dots, weak staining can be detected surrounding a bile canaliculus. (*A*) Bar, 50 μm; ×200. (*B*) Bar, 10 μm; ×800.

of rat liver, heart, and fibroblast (rat 3Y1 cells) in the high-molecular weight region was analyzed by 4% PAGE, in all tissues a polypeptide with only the same molecular weight as tenuin was clearly identified (Fig. 3 *A*). Judging from the mobility of α-, β-connectin (titin) (20, 22, 34) and myosin heavy chain, the molecular weight of tenuin was estimated to be ∼400 kD. When the electrically phoresed samples were transferred to nitrocellulose and reacted for AJ-0222 or AJ-12249, clear staining of polypeptide at ∼400 kD was observed in all tissues examined (Fig. 3 *B*). As shown in lane 3 in Fig. 3 *B*, tenuin can be detected in whole liver as a single band, indicating that gross proteolysis does not occur during the isolation of adherens junctions.

Microscopic Localization of Tenuin in Various Types of Cells

Using AJ-0222 or AJ-12249, frozen sections of various types of cells bearing adherens junctions were examined by immunofluorescence microscopy to study the distribution of the antigen. Both mAbs stained all types of cells examined in the same pattern. In the liver, characteristic staining of the junctional complex region was revealed (Fig. 4, *A* and *B*). In the longitudinal-section view of each bile canaliculus, a pair of parallel continuous lines was visible; in cross-section, a pair of intensively stained dots and weak staining around the canaliculus were observed (Fig. 4 *B*). To interpret these images, we have attempted to apply our anti-tenuin mAbs to the cryo-ultrathin sections at electron microscopic level. However, we faced a technical difficulty; when the samples were fixed with >2% formaldehyde, our anti-

bodies showed no specific staining pattern, indicating that postsectioning labeling with our antibodies was very difficult. Therefore, isolated bile canaliculi-enriched fraction was used to doubly immunolocalize tenuin and vinculin at the electron microscopic level (Fig. 5). Because the sample was fixed only with 1% formaldehyde before antibody labeling, the preservation of the isolated bile canaliculi was not perfect; for example, the actin bundles surrounding bile canaliculi mostly disappeared. However, by the use of this preparation, it was clearly shown that mAbs specific to tenuin mainly labeled the cytoplasmic side of the adherens junction, which was identified by the vinculin-labeling (Fig. 5, *A* and *C*). Desmosomes were by no means labeled by anti-tenuin and anti-vinculin (Fig. 5 *D*). In the isolated bile canaliculi in which the actin bundle underlying the plasma membrane was "fortuitously" preserved, the actin bundle was weakly but clearly labeled (Fig. 5 *B*). Together, it may be safe to say that in the liver, tenuin is enriched in the undercoat of adherens junctions and may also occur in the actin bundles associated with the junction. To confirm this conclusion, by the use of isolated bile canaliculi, we have further compared the distribution of tenuin with that of actin, vinculin, and desmoplakin I/II at immunofluorescence microscopic level (Fig. 6). Because in this preparation the actin bundles surrounding bile canaliculi were not preserved, both rhodamine phalloidin and anti-vinculin antibody stained two belts of adherens junctions in the same pattern for each bile canaliculus. The staining pattern of tenuin completely coincided with that of actin and vinculin (Fig. 6, *A–D*). In sharp contrast, the staining pattern of desmoplakin I/II was short linear or
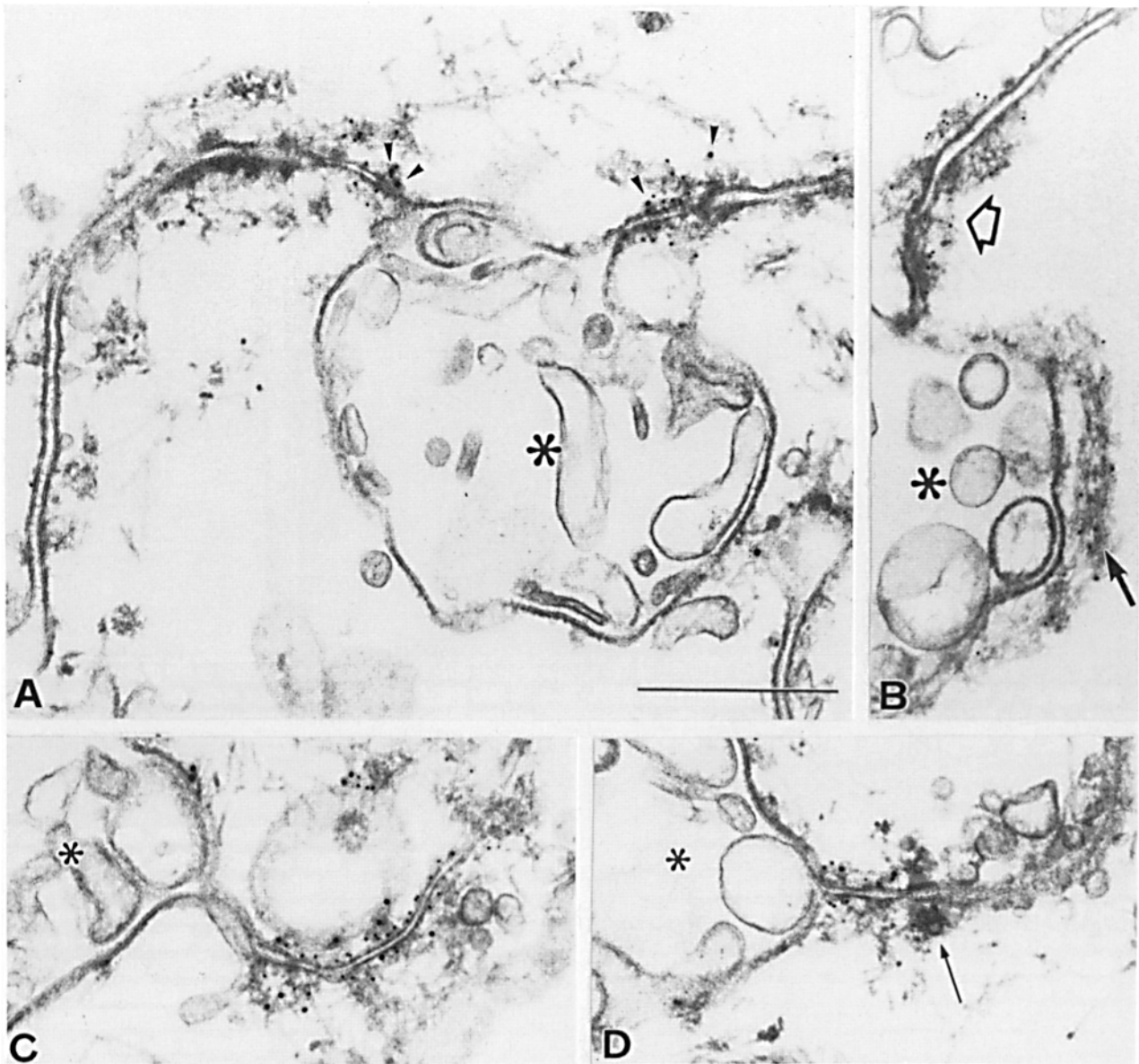
Figure 5. Dual-label immunoelectron micrographs of the isolated bile canaliculi- (∗) enriched fraction with mouse anti–tenuin (AJ-0222) and rabbit anti–rat vinculin. As second antibodies, goat anti–mouse IgM coupled to 10 nm gold (GAMIgM G10) and goat anti–rabbit IgG coupled to 15 nm gold (GARIgG G15) are used. Only *B* is labeled singly with AJ-0222 followed by GAMIgM G10. The samples are fixed with 1% formaldehyde for 10 min before immunolabeling. (*A* and *C*) mAb specific to tenuin (10 nm gold) mainly labels the cytoplasmic side of the adherens junction, which can be identified by the vinculin labeling (15 nm gold; *arrowheads* in *A*). (*D*) Desmosome (*arrow*) is not labeled by anti–tenuin (10 nm gold) and anti–vinculin (15 nm gold). (*B*) In the isolated bile canaliculus in which the actin bundle underlying the plasma membrane is "fortuitously" preserved, the actin bundle (*small arrow*) as well as the adherens junctions (*large arrow*) are labeled with anti–tenuin (10 nm gold). Bar, 0.5 μm; ×60,000.

patchy, and did not overlap with that of tenuin (Fig. 6, *E* and *F*).

When frozen sections of rat intestine were used, both AJ-0222 and AJ-12249 clearly stained the apical portion of the epithelial cells in the same pattern (Fig. 7, *A* and *B*). In oblique section, belt-like or circumferential staining was seen around the apical pole of each epithelial cell (Fig. 7 *C*). The staining patterns of cardiac muscle cells with these two antibodies were similar. Extensive labeling of the intercalated discs was clearly observed (Fig. 7, *D* and *E*).

To further analyze the occurrence of tenuin in the actin

bundles in nonmuscle cells, the cultured fibroblasts (rat 3Y1 cells) and MDBK epithelial cells were examined by immunofluorescence microscopy. In 3Y1 cells, the stress fibers were brightly stained (Fig. 8, *A* and *B*). When 3Y1 cells were doubly stained with anti–tenuin and anti–vinculin antibodies, it was revealed that tenuin was actually localized at the cell-to-substrate adherens junctions (focal contacts) in addition to the stress fibers (Fig. 8, *C* and *D*). Although the staining intensity was not even along the single stress fibers, no periodic staining patterns were observed. Even when the localization of tenuin in the stress fiber was analyzed at the
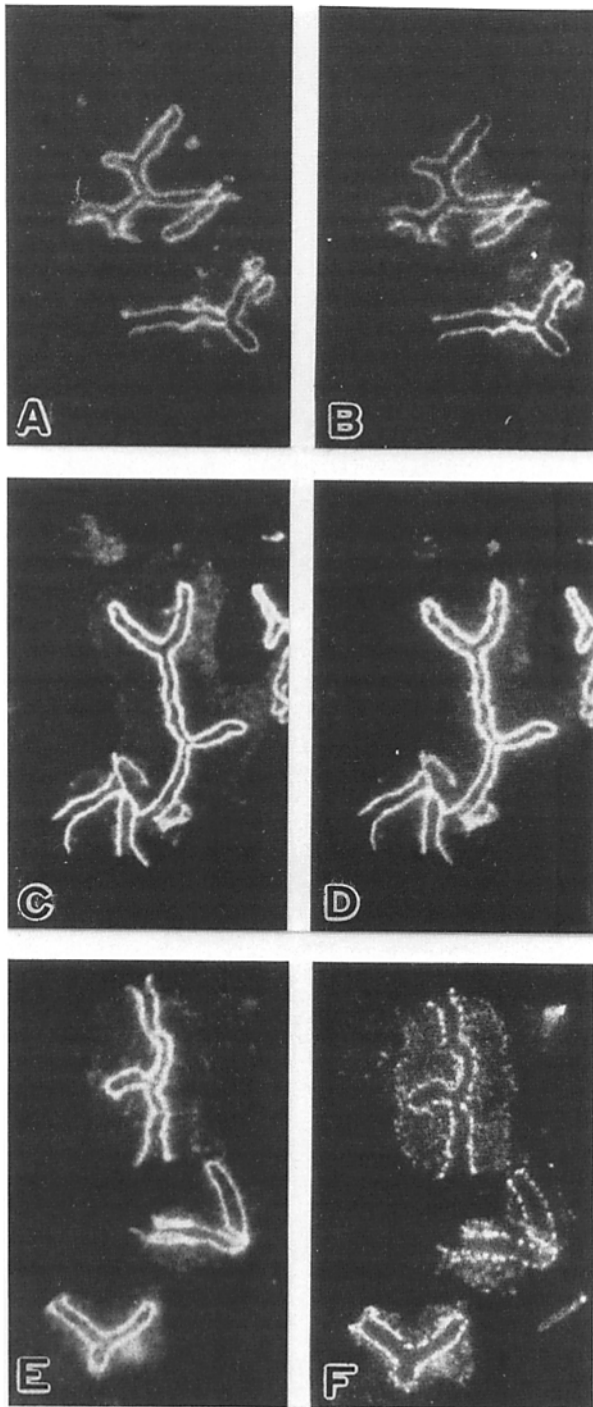
Figure 6. Localization of tenuin, actin, vinculin, and desmoplakin I/II in the isolated bile canaliculi. (*A* and *B*) Dual-label immunofluorescence micrographs with anti-tenuin (*A*) and rhodamine-phalloidin (*B*; localization of actin). (*C* and *D*) Dual-label immunofluorescence micrographs with anti-tenuin (*C*) and anti-vinculin (*D*). (*E* and *F*) Dual-label immunofluorescence micrographs with anti-tenuin (*E*) and anti-desmoplakin I/II (*F*). The staining patterns of tenuin completely coincide with those of actin and vinculin, whereas the staining pattern of desmoplakin is short linear, or patchy and does not overlap with that of tenuin. Bar, 10 μm; ×900.

electron microscopic level, no periodicity was ever detected (Fig. 9). When the fluorescently-labeled MDBK cells were observed at ventral focal planes, the stress fibers were clearly visualized; at the apical focal planes, the circumferential actin bundles were stained (Fig. 10, *A* and *B*). The localization of tenuin at the circumferential actin bundles was further confirmed at electron microscopic level (data not shown).

Discussion

In this study, we have successfully obtained three types of mAbs specific to a new high-molecular weight protein which was identified in the cell-to-cell adherens junction. This protein, called tenuin here (from Latin 'tenuis', thin or slender), with a molecular mass of ~400 kD, was shown by immune blot analyses to occur in various types of cells. Immunofluorescence microscopy and immune electron microscopy have revealed that tenuin is distributed not only in the undercoat of adherens junctions but also at the actin bundles in nonmuscle cells such as stress fibers in cultured fibroblasts and circumferential bundles in epithelial cells.

So far, several proteins have been reported to be located at the undercoat of adherens junctions: α-actinin (18), filamin (9), vinculin (7, 10), talin (1, 2), plakoglobin (4), radixin (31), etc. Among them, vinculin, talin, and radixin are localized exclusively at the undercoat, whereas α-actinin and filamin are distributed both at the undercoat and at the actin bundles associated with adherens junctions. Judging from the results obtained here, tenuin can be categorized as the latter type. However, in sharp contrast to the observations that α-actinin- and filamin-specific staining showed a typically spotty or patchy pattern associated with stress fibers at both light and electron microscopic levels (17, 18), tenuin-specific staining was almost homogeneously localized along stress fibers. In this sense, tenuin is unique among the proteins associated with stress fibers. The characteristic molecular shape of tenuin has persuaded us to consider the physiological roles of this protein. Recently, it has been shown that connectin (or titin) plays an important role in forming and keeping the structural integrity of myofibrils in skeletal muscle, and that its molecule looks like a fairly long thin strand (20-23, 34, 35). Connectin (or titin) has never been identified in nonmuscle cells. Therefore, it is fascinating to speculate that tenuin plays a crucial role in forming and maintaining actin filament bundles in nonmuscle cells. Although it is still premature to further discuss the physiological roles of tenuin in nonmuscle cells, we believe further studies of the in vitro and in vivo nature of tenuin will shed light on the molecular mechanism of the formation and destruction of stress fibers.

Recently, a new high-molecular weight protein, designated zeugmatin, has been identified from cardiac muscle cells using mAb techniques, and shown to be localized at Z bands and intercalated discs (adherens junctions) in cardiac muscle cells (19). Although both zeugmatin and tenuin are distributed in the intercalated discs, these two high-molecular weight proteins appear to be distinct from each other: the molecular weight of zeugmatin is larger than that of tenuin (see Fig. 10 in reference 19) and tenuin is not localized at Z-bands. Another high-molecular weight protein that can be compared with tenuin is 'dystrophin', which has been recently identified in studies of Duchenne muscular dystrophy
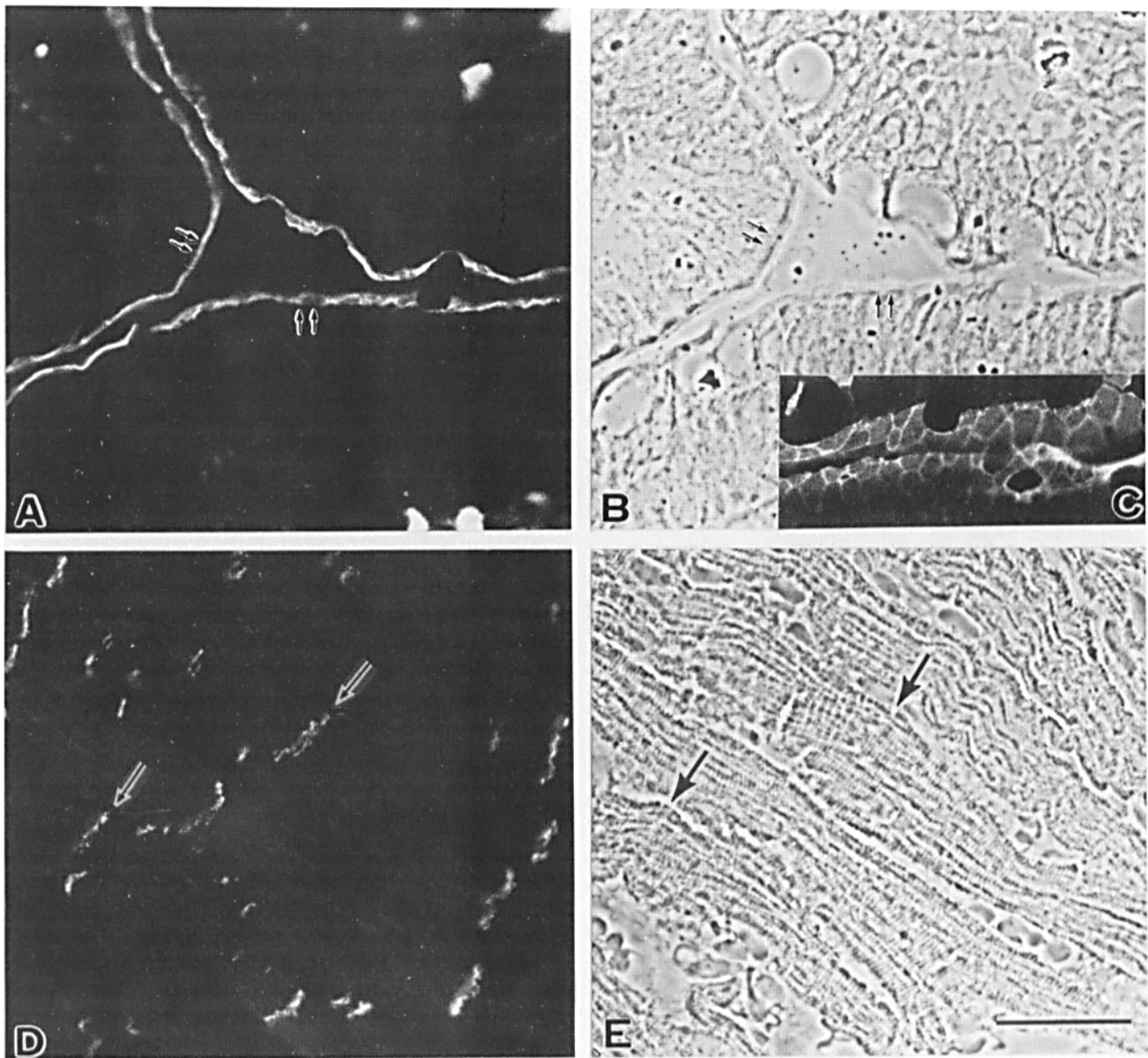
Figure 7. Localization of tenuin in rat intestine (*A–C*) and heart (*D* and *E*). Indirect immunofluorescence images with AJ-12249 (*A, C, D*) and phase contrast images (*B* and *E*). (*A–C*) AJ-12249 strongly stains the apical portion of the epithelial cells (*arrows*). In an obliquely cut section (*C*), the tenuin staining is localized in the cell-to-cell boundary. (*D* and *E*) Extensive staining of AJ-12249 is detected in the intercalated discs (*arrows*). Bar, 100 μm; ×200.

(12). This protein has a similar molecular mass (~400 kD) to tenuin. However, because tenuin occurs in *mdx* mice, which lack the dystrophin gene (data not shown), we can say that tenuin is a different protein from dystrophin.

In the previous paper, we reported succeeding in isolating the cell-to-cell adherens junctions from rat liver and in finding α-actinin, vinculin, actin, and seven unidentified polypeptides in the undercoat of the junction (30). Among them, three major polypeptides are in the molecular mass range of >200 kD. In addition, four minor bands can be identified in this molecular weight range. In this study, tenuin, the protein with the highest molecular weight in this group, has been characterized. The question of the chemical nature of the other high-molecular weight polypeptides has naturally arisen. Studies along this line are currently being conducted in our laboratory.
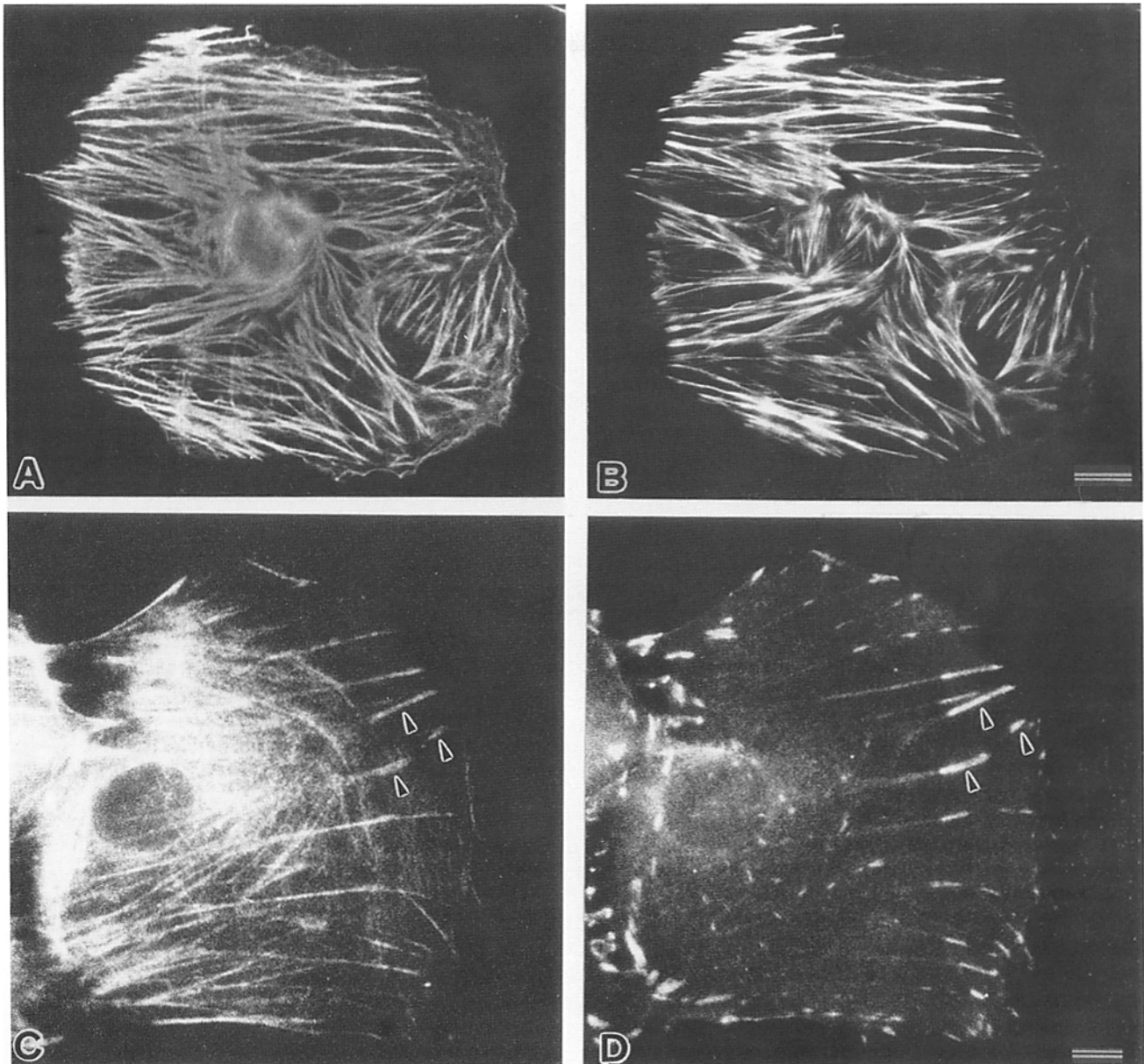
Figure 8. Indirect immunofluorescence micrographs with anti-tenuin of rat cultured fibroblasts (3Y1 cells). (*A* and *B*) Double staining with AJ-12249 (*A*) and rhodamine-phalloidin (*B*). The stress fibers are brightly stained both by AJ-12249 and phalloidin. Bar, 50 µm; ×170. (*C* and *D*) Double staining with AJ-12249 (*C*) and rabbit anti-vinculin (*D*). Tenuin is localized at the cell-to-substrate adherens junctions (*arrowheads*). Bar, 10 µm; ×800.

References

1. Burridge, K., and L. Connell. 1983. A new protein of adherens plaques and ruffling membranes. *J. Cell Biol.* 97:359–367.
2. Burridge, K., and P. Mangeat. 1984. An interaction between vinculin and talin. *Nature (Lond.).* 308:744–746.
3. Byers, H. R., G. E. White, and K. Fujiwara. 1984. Organization and function of stress fibers in cells in vitro and in situ. *Cell Muscle Motil.* 5:83–137.
4. Cowin, P., H.-P. Kapprell, W. W. Franke, J. Tamkun, and R. O. Hynes. 1986. Plakoglobin: a protein common to different kinds of intercellular adhering junctions. *Cell.* 46:1063–1073.
5. De Blas, A. L., and H. M. Cherwinski. 1983. Detection of antigens on nitrocellulose paper. Immunoblots with monoclonal antibody. *Anal. Biochem.* 133:214–219.
6. Farquhar, M. G., and G. E. Palade. 1963. Junctional complexes in various epithelia. *J. Cell Biol.* 17:375–409.
7. Geiger, B. 1979. A 130k protein from chicken gizzard: its localization at the termini of microfilament bundles in cultured chicken cells. *Cell.* 18:193–205.
8. Geiger, B. 1983. Membrane-cytoskeletal interaction. *Biochim. Biophys. Acta.* 737:305–341.
9. Geiger, B., Z. Avenur, G. Rinnerthaler, H. Hinssen, and V. J. Small. 1984. Microfilament-organizing centers in areas of cell contact: cytoskeletal interactions during cell attachment and locomotion. *J. Cell Biol.* 99:83s–91s.
10. Geiger, B., K. T. Tokuyasu, A. H. Dutton, and S. J. Singer. 1980. Vinculin, an intracellular protein localized at specialized sites where microfilament bundles terminate at cell membranes. *Proc. Natl. Acad. Sci. USA.* 77:4127–4131.
11. Geiger, B., T. Volk, and T. Volberg. 1985. Molecular heterogeneity of adherens junctions. *J. Cell Biol.* 101:1523–1531.
12. Hoffman, E. P., R. H. Brown, Jr., and L. M. Kunkel. 1987. Dystrophin: the protein product of the Duchenne muscular dystrophy locus. *Cell.* 51:919–928.
13. Isenberg, G., P. C. Rathke, N. Hulsmann, W. W. Franke, and K. E. Wahlfarth-Bottermann. 1976. Cytoplasmic actomyosin fibers in tissue culture cells. Direct proof of contractility by visualization of ATP-induced contraction in fibrils isolated by laser micro-beam dissection. *Cell. Tiss. Res.* 166:427–443.
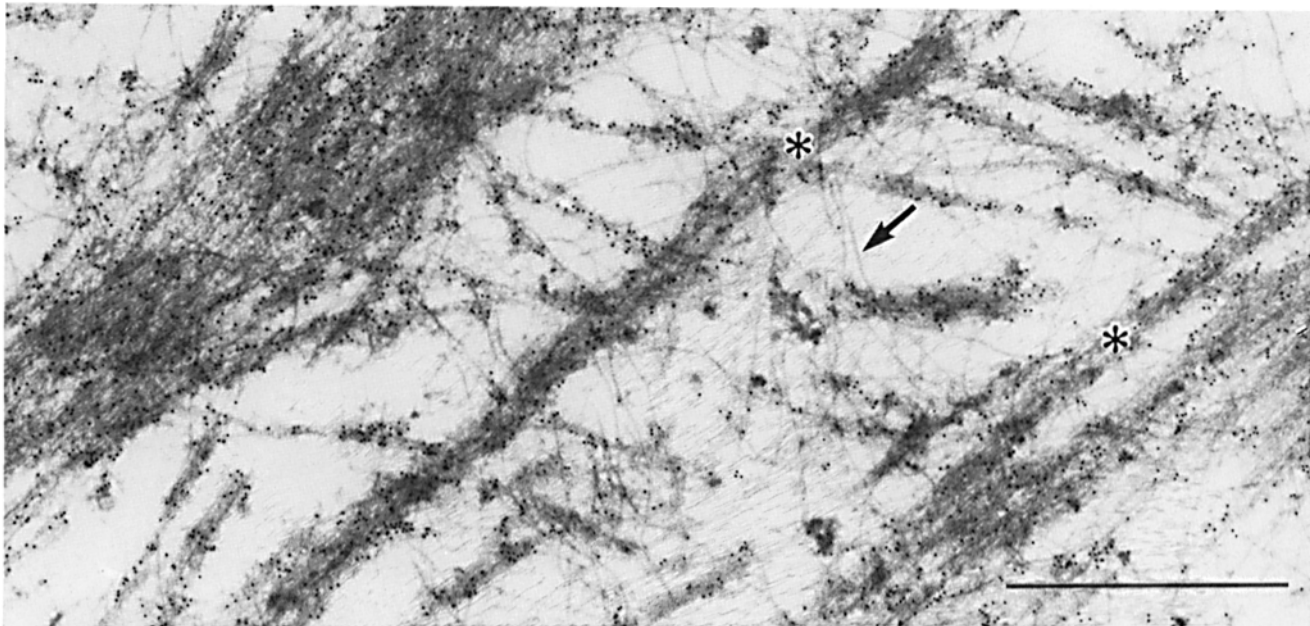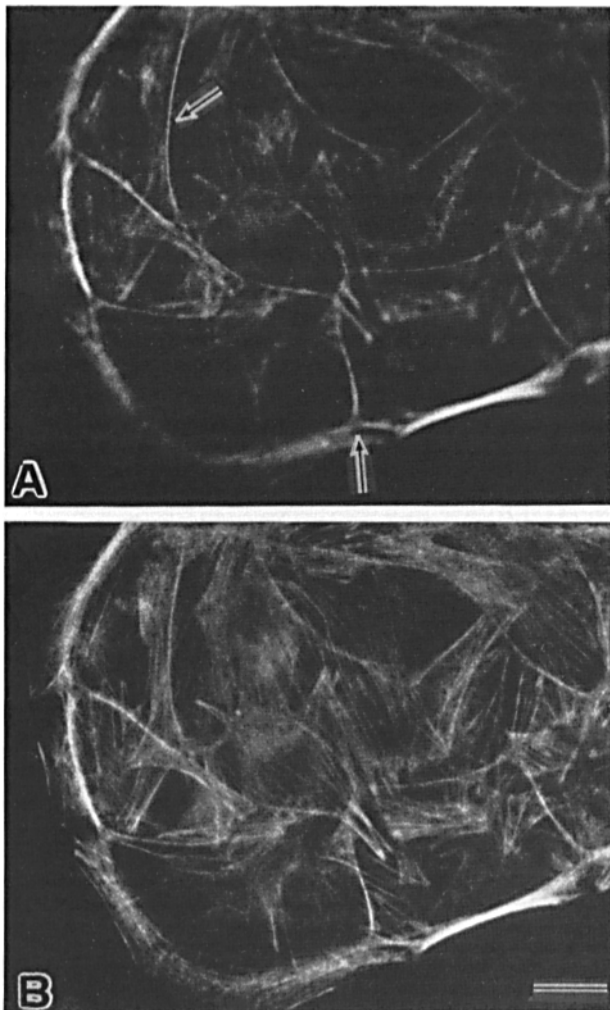
Figure 9. Immunoelectron micrographs with anti-tenuin (AJ-12249) of rat cultured fibroblasts (3Y1 cells). The stress fibers (*) are heavily decorated, whereas only a few gold particles are detected on 10-nm filaments (*arrows*). No periodicity in labeling pattern along the stress fiber is detected. Bar, 1 μm; ×36,000.

14. Ishikawa, H. 1979. Identification and distribution of intracellular filaments. *In* Cell Motility: Molecules and Organization. S. Hatano, H. Ishikawa, and H. Sato, editors. University of Tokyo Press, Tokyo. 417–444.
15. Köhler, G., M. Schreier, H. Hengartner, C. Berek, M. Trucco, L. Forni, T. Staehelin, J. Stocker, and B. Takass. 1980. Hybridoma Techniques. Cold Spring Harbor Laboratory, Cold Spring Harbor, NY. 65.
16. Laemmli, U. K. 1970. Cleavage of structural proteins during the assembly of the head of bacteriophage T4. *Nature (Lond.).* 227:680–685.
17. Langanger, G., J. De Mey, M. Moeremans, G. Daneels, M. De Brabander, and J. V. Small. 1984. Ultrastructural localization of α-actinin and filamin in cultured cells with the immunogold staining (IGS) method. *J. Cell Biol.* 99:1324–1334.
18. Lazarides, E., and K. Burridge. 1975. α-actinin: immunofluorescent localization of a muscle structural protein in nonmuscle cells. *Cell.* 6:289–298.
19. Maher, P. A., G. F. Cox, and S. J. Singer. 1985. Zeugmatin: a new high molecular weight protein associated with Z lines in adult and early embryonic striated muscle. *J. Cell Biol.* 101:1871–1883.
20. Maruyama, K., S. Kimura, K. Ohashi, and Y. Kuwano. 1981. Connectin, an elastic protein of muscle: identification of titin with connectin. *J. Biochem. (Tokyo).* 89:701–709.
21. Maruyama, K., S. Kimura, H. Yoshidomi, H. Sawada, and M. Kikuchi. 1984. Molecular size and shape of α-connectin, an elastic protein of striated muscle. *J. Biochem. (Tokyo).* 95:1423–1433.
22. Maruyama, K., S. Matsubara, R. Natori, Y. Nonomura, S. Kimura, K. Ohashi, F. Murakami, S. Handa, and G. Eguchi. 1977. Connectin, an elastic protein of muscle: Characterization and function. *J. Biochem. (Tokyo).* 82:317–337.
23. Maruyama, K., H. Sawada, S. Kimura, K. Ohashi, H. Higuchi, and Y. Umazume. 1984. Connectin filaments in stretched skinned fibers of frog skeletal muscle. *J. Cell Biol.* 99:1391–1397.
24. Owaribe, K., and H. Masuda. 1982. Isolation and characterization of circumferential microfilament bundles from retinal pigmented epithelial cells. *J. Cell Biol.* 95:310–315.
25. Pollard, T. D., and R. R. Weihing. 1974. Actin and myosin in cell movement. *CRC Crit. Rev. Biochem.* 2:1–65.
26. Rohrschneider, L. R. 1980. Adhesion plaque of Rous sarcoma virus-transformed cells contain the src gene product. *Proc. Natl. Acad. Sci.*

Figure 10. Localization of tenuin (AJ-12249) in cultured Madin Darby bovine kidney (MDBK) epithelial cells. (*A* and *B*) Indirect immunofluorescence micrographs with AJ-12249. At the apical focal planes (*A*), the circumferential actin bundles (*arrows*) are stained, while at the ventral focal planes (*B*) the stress fibers are clearly visualized. Bar, 50 μm; ×200.

USA. 77:3514–3518.

27. Sanger, J. M., B. Mittal, and J. W. Sanger. 1985. Structure and assembly of microfilament bundles. *In* Cell Motility: Mechanism and Regulation. H. Ishikawa, S. Hatano, and H. Sato, editors. University of Tokyo Press, Tokyo. 461–475.

28. Shriver, K., and L. Rohrschneider. 1981. Organization of pp60[src] and selected cytoskeletal proteins within adhesion plaques and junctions of Rous sarcome virus-transformed rat cells. *J. Cell Biol.* 89:525–535.

29. Staehelin, A. 1974. Structure and function of intercellular junctions. *Int. Rev. Cytol.* 39:191–283.

30. Tsukita, S., and S. Tsukita. 1989. Isolation of cell-to-cell adherens junctions from rat liver. *J. Cell Biol.* 108:31–41.

31. Tsukita, S., Y. Hieda, and S. Tsukita. 1989. A new 82 kD-barbed end capping protein (radixin) localized in the cell-to-cell adherens junction: Purification and characterization. *J. Cell Biol.* 108:2369–2382.

32. Tyler, J. M., and D. Branton. 1981. Rotary shadowing of extended molecules dried from glycerol. *J. Ultrastruct. Res.* 71:95–102.

33. Vassen, R. T. M. J., J. Kreike, and G. S. P. Groot. 1981. Protein transfer to nitrocellulose filters. A simple method for quantitation of single proteins in complex mixtures. *FEBS (Fed. Eur. Biochem. Soc.) Lett.* 124:193–196.

34. Wang, K., J. McClure, and A. Tu. 1979. Titin: major myofibrillar component of striated muscle. *Proc. Natl. Acad. Sci. USA.* 76:3698–3702.

35. Wang, K., and R. Ramirez-Mitchell. 1983. A network of transverse and longitudinal intermediate filaments is associated with sarcomeres of adult vertebrate skeletal muscle. *J. Cell Biol.* 96:562–570.

36. Wessells, N. K., B. S. Spooner, J. F. Ash, M. O. Bradley, M. A. Luduena, E. L. Tayler, J. T. Wrenn, and K. M. Yamada. 1971. Microfilaments in cellular and developmental processes. Contractile microfilament machinery of many cell types is reversibly inhibited by cytochalasin B. *Science (Wash. DC).* 171:135–143.